Reorientation of the CCl_3 Group in Chloral 4-Chlorobenzylhemiacetal. A Pulsed ^{35}Cl NQR and X-ray Study *

Masao Hashimoto, Takahiro Isono, and Noriko Yomesaka
Department of Chemistry, Faculty of Science, Kobe University, Nadaku, Kobe 657, Japan

Haruo Niki
Department of Physics, Division of General Education, University of the Ryukyus, Nishihara, Okinawa 903-01, Japan

Hiroshi Kyan and Takeshi Hamagawa
Department of Physics, College of Science, University of the Ryukyus, Nishihara, Okinawa 903-01, Japan

Z. Naturforsch. **47a**, 293–298 (1992); received July 25, 1991

The crystal structure of the title compound was determined at 291 K: monoclinic, space group C^5_{2h}-$P2_1/n$, $Z=4$, $a=1693.2(1)$, $b=579.3(1)$, $c=1232.5(1)$ pm, and $\beta=107.21(1)°$, $R=0.0415$. A sharp decrease of T_1 of Cl NQR found at $T \gtrsim 270$ K for the CCl_3 group is attributed to the reorientation of the group over a potential barrier of ca. 50 kJ/mol. Intermolecular interactions between the CCl_3 and the neighboring atoms seem to dominate the magnitude of the potential barrier. T_1^{-1} of the ^{35}Cl NQR of the Cl atom on the benzene ring obeyed the T^2 law well in the range $80 \lesssim T/K \lesssim 270$, while at $T \gtrsim 280$ K it deviated from the T^2 law.

Key words: Crystal structure, Hydrogen bond, Chlorine NQR, Spin lattice relaxation, Atom-atom potential method.

Introduction

It is often observed for trichloromethyl derivatives that the spin lattice relaxation time (T_1) of Cl NQR corresponding to the CCl_3 group drops sharply with increasing temperature in a certain temperature range far below the melting point. The phenomenon has been attributed to the fluctuations of the electric field gradient (EFG) caused by the reorientation of the CCl_3 group. For a number of compounds, the magnitude of the potential barrier height (V_0) hindering the reorientation have been determined from the temperature dependence of T_1 [1]. In many cases, however, the origin of the barrier height is unknown. For a few compounds of known crystal structure we applied the atom-atom potential method to estimate the value of V_0 and found its dependence on intermolecular contributions [2, 3].

In the present work we determined the crystal structure of chloral 4-chlorobenzylhemiacetal ($Cl_3CCH(OH)O \cdot CH_2C_6H_4Cl$, pCB-CH), and measured the relaxation times of the ^{35}Cl NQR to study molecular motions in the crystal.

In chloral n-butylhemiacetal (nB-CH) and chloral cyclohexylhemiacetyl (cycHx-CH), a dynamic disorder of hydrogen atoms in the OH groups seems to affect the Cl T_1 of the CCl_3 groups [4, 5]. The possibility of the disorder in pCB-CH will be examined in this article.

Experimental

Preparation

Chloral 4-chlorobenzylhemiacetal (pCB-CH) was prepared from chloral and 4-chlorobenzylalcohol by the method described in [6] and purified by recrystallizations from petroleum ether.

^{35}Cl NQR

The spin-lattice relaxation time (T_1), spin-spin relaxation time (T_2), and inverse line width parameter

---

* Presented at the XIth International Symposium on Nuclear Quadrupole Resonance Spectroscopy, London, United Kindom, July 15–19, 1991.

Reprint requests to Dr. Masao Hashimoto, Department of Chemistry, Faculty of Science, Kobe University, Nadaku, Kobe 657, Japan.

(T_2^*) of Cl NQR were measured by a conventional pulse spectrometer reported in [4].

In the lower temperature range, where T_1 was longer than T_2, T_1 was determined by the $90°-\tau-90°-\tau'-180°$ pulse sequence, while at higher temperatures the $90°-\tau-90°$ pulse method was applied. T_2 was measured with the usual $90°-\tau-180°$ pulse sequence. T_2^*, which was defined as the time required for a given induction signal to decay to $1/e$ of its maximum value, was obtained from the shapes of free induction decays or from those of echo signals. The widths of 90° pulses were 10 to 15 µs.

Crystal Structure Analysis

The crystal structure of pCB-CH was determined by the single crystal technique at room temperature using MoKα radiation. The experimental details are given in Table 1. The crystal structure was solved by the direct method MULTAN 78 [7] and refined by the least-squares method (HBLS-V) with anisotropic and isotropic temperature factors for non-hydrogen and hydrogen atoms, respectively [8]. All calculations were performed on an ACOS 1000 Computer at the Information Processing Center of Kobe Unversity with the UNICS systems [9].

Table 1. Experimental conditions for the crystal structure determination and crystalographic data of chloral 4-chlorobenzylhemiacetal.

Formula		$C_9H_8Cl_4O_2$
Molar mass, g/mol		290.0
Crystal habitus		needle
Size/mm^3		$0.3 \times 0.2 \times 0.1$
Diffractometer		Rigaku AFC-5
Wavelength, λ/pm		71.073 (MoKα)
$(\sin\theta/\lambda)_{max}$/pm^{-1}		0.00595
Monochromator		graphite
Temperature, T/K		291
Linear absorption coefficient, μ/m^{-1}		1005
Lattice constants	a/pm	1693.2(1)
	b/pm	579.3(1)
	c/pm	1232.5(1)
	β/°	107.21(1)
Volume of the unit cell $V \cdot 10^{-6}$/pm^3		1154.8(1)
Space group		C_{2h}^5-$P2_1/n$
Formula units/unit cell		$Z=4$
d_{calc}/(Mg · m^{-3})		1.668
d_{obs}/(Mg · m^{-3})		1.676
Scan		$2\theta-\omega$
Number of measured reflections		2396
Symmetry independent reflections		2041
Reflections considered		1588
Number of free parameters		169
$F(000)$		584
$R(F)$		0.0415
$R_w(F)$		0.0471

Point positions. All atoms in 4e:

$x, y, z;$ $\frac{1}{2}+\bar{x}, \frac{1}{2}+y, \frac{1}{2}+\bar{z}$
$\bar{x}, \bar{y}, \bar{z};$ $\frac{1}{2}+x, \frac{1}{2}+\bar{y}, \frac{1}{2}+z$

Infrared (IR) Spectrum

IR spectra were recorded on a Hitachi EPI-G2 spectrometer at various temperatures with the aid of a conventional cryostat described in [10].

Results

Crystal Structure of pCB-CH

In Table 1 the crystallographic data of pCB-CH are given. Table 2 lists the positional and thermal parameters of the atoms in the asymmetric unit of the crystal.

It should be noted that a difference Fourier map showed a diffuse electron distribution corresponding to the hydrogen of the OH group (H1). When a least-squares calculation was performed with H1 located tentatively in two different positions at the fractional coordinates (0.710, −0.384, 0.748 and 0.754, −0.425, 0.793) with weights of 0.7 and 0.3, respectively, the R factors were almost unchanged ($R=0.0414$ and $R_w=0.0469$) but the temperature factors became better (4.2 and 3.3, respectively) than that of H1 given in Table 2.

The bond lengths and bond angles are given in Figs. 1 and 2. These values show no unusual features. The molecular packing projected along the b-axis onto the (ac) plane is shown in Figure 3.

^{35}Cl NQR

The temperature dependence of T_1 and T_2 of the Cl NQR are shown in Figure 4. Three resonance lines (ν_{2-4}) faded out at about 330 K, while ν_1 was still detectable at 363 K (mp = 370 K). The ^{35}Cl NQR frequencies of the four lines (ν_{1-4}) at 90 K were $\nu_1 = 34.301$, $\nu_2 = 38.547$, $\nu_3 = 38.826$, and $\nu_4 = 39.442$ MHz. The lowest frequency line (ν_1) corresponds to the Cl atom on the benzene ring (Cl4 in Figure 1).

The T_2^*, of ν_{1-4} were in the range of 30 to 120 µs, indicating that lattice imperfections dominate the widths of the NQR lines.

Infrared (IR) Spectrum

The IR band assigned to the OH stretching vibration was broad and seemed to have two components

Table 2. Positional and thermal parameters (with standard deviations) of chloral 4-chlorobenzylhemiacetal. The temperature factor exponent has the form: $-(B_{11} \cdot h^2 + B_{22} \cdot k^2 + B_{33} \cdot l^2 + B_{12} \cdot hk + B_{13} \cdot hl + B_{23} \cdot kl)$ for non-hydrogen atoms, $-B_{\text{iso}} \sin^2 \theta / \lambda^2$ for hydrogen atoms. The temperature factors (B_{nm}) are given in units of $(10^{-10}\ \text{m})^2$.

Atom	x/a	y/b	z/c	B_{11} or B_{iso}	B_{22}	B_{33}	B_{12}	B_{13}	B_{23}
Cl1	0.8246(1)	0.0890(2)	0.9847(1)	0.0045(0)	0.0192(2)	0.0062(1)	0.0022(2)	0.0031(1)	−0.0017(2)
Cl2	0.7855(1)	−0.3643(2)	1.0489(1)	0.0047(0)	0.0301(3)	0.0067(1)	−0.0025(2)	0.0061(1)	0.0035(3)
Cl3	0.9511(1)	−0.2579(2)	1.0515(1)	0.0030(0)	0.0405(4)	0.0108(1)	0.0051(2)	0.0018(1)	0.0025(3)
Cl4	1.1580(1)	0.3257(2)	0.6119(1)	0.0042(0)	0.0450(4)	0.0107(1)	−0.0095(2)	0.0076(1)	−0.0054(4)
O1	0.8744(2)	−0.1555(4)	0.8061(2)	0.0067(1)	0.0229(8)	0.0086(2)	−0.0056(6)	0.0111(3)	−0.0064(7)
O2	0.7425(2)	−0.2571(5)	0.8011(2)	0.0048(1)	0.0328(9)	0.0055(2)	−0.0032(6)	0.0013(3)	−0.0021(7)
C1	0.8462(2)	−0.2088(6)	0.9790(3)	0.0029(1)	0.0208(11)	0.0055(3)	0.0007(6)	0.0030(3)	0.0013(9)
C2	0.8269(2)	−0.2911(6)	0.8558(3)	0.0041(2)	0.0204(11)	0.0059(3)	−0.0024(7)	0.0047(3)	−0.0008(9)
C3	0.9013(2)	−0.2698(7)	0.7201(3)	0.0048(2)	0.0345(15)	0.0074(3)	−0.0064(9)	0.0067(4)	−0.0113(11)
C4	0.9652(2)	−0.1234(6)	0.6923(3)	0.0033(1)	0.0265(12)	0.0049(3)	−0.0028(7)	0.0033(3)	−0.0046(9)
C5	0.9435(2)	0.0818(7)	0.6334(3)	0.0026(1)	0.0331(13)	0.0068(3)	0.0006(7)	0.0029(3)	−0.0013(11)
C6	1.0018(2)	0.2221(6)	0.6085(3)	0.0034(1)	0.0278(12)	0.0064(3)	0.0024(7)	0.0032(3)	−0.0018(10)
C7	1.0836(2)	0.1514(7)	0.6429(3)	0.0031(1)	0.0325(13)	0.0060(3)	−0.0030(7)	0.0044(3)	−0.0044(10)
C8	1.1069(2)	−0.0524(7)	0.7002(3)	0.0029(1)	0.0342(14)	0.0068(3)	0.0010(7)	0.0027(3)	−0.0025(11)
C9	1.0474(2)	−0.1880(7)	0.7253(3)	0.0039(2)	0.0301(13)	0.0059(3)	0.0009(7)	0.0026(4)	0.0018(10)
H1	0.7246(32)	−0.3905(99)	0.7607(48)	8.2					
H2	0.8405(18)	−0.4551(59)	0.8540(27)	1.2					
H3	0.8488(23)	−0.2962(71)	0.6498(34)	3.5					
H4	0.9218(27)	−0.4266(83)	0.7466(38)	5.5					
H5	0.8876(21)	0.1264(64)	0.6100(30)	2.7					
H6	0.9866(21)	0.3680(64)	0.5657(30)	2.5					
H7	1.1630(24)	−0.1091(75)	0.7168(34)	4.1					
H8	1.0644(19)	−0.3253(59)	0.7685(28)	1.6					

at ca. 290 K. At lower temperatures, the band was found to split into two components (3446 and 3395 cm^{-1} at ca. 220 K and 3437 and 3376 cm^{-1} at ca. 80 K). The relative intensity of the lower wavenumber component became markedly stronger than that of the other at lower temperatures. The OD stretching band in the deuterated pCB-CH exhibited the same feature.

Discussion

Crystal Structure

The crystal structure of pCB-CH is characterized by chains of O–H ··· O hydrogen bond running along a 2_1 axis. Since the acetal oxygen (–O–) and the OH group can act as the hydrogen bond acceptor, the crys-

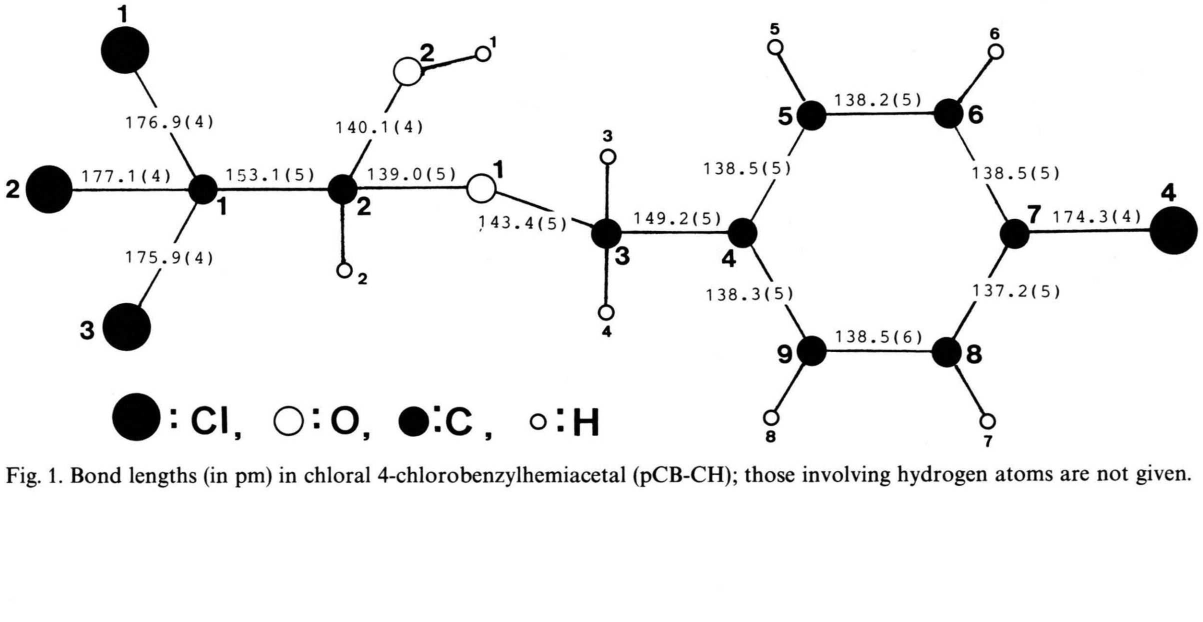

Fig. 1. Bond lengths (in pm) in chloral 4-chlorobenzylhemiacetal (pCB-CH); those involving hydrogen atoms are not given.

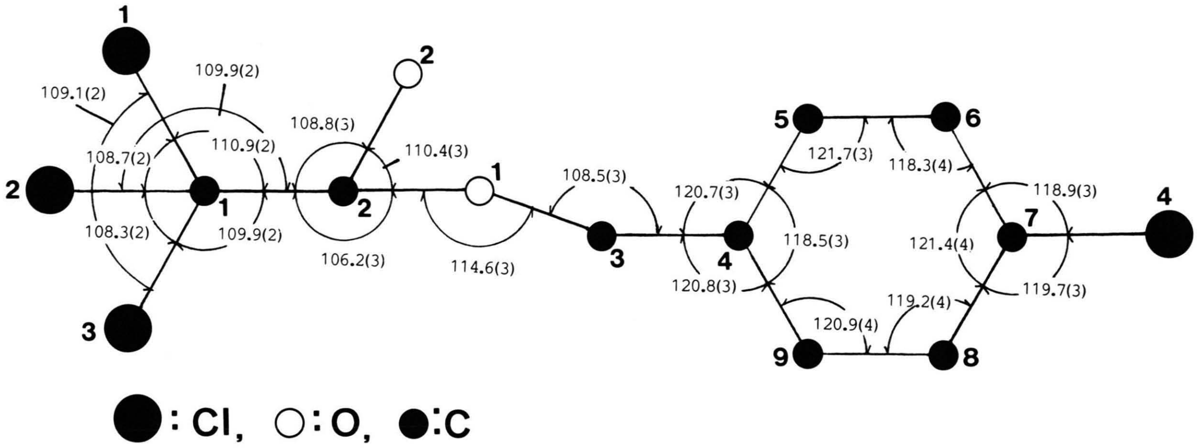

Fig. 2. Bond angles (in angular degrees) in pCB-CH. The hydrogen atoms are not shown.

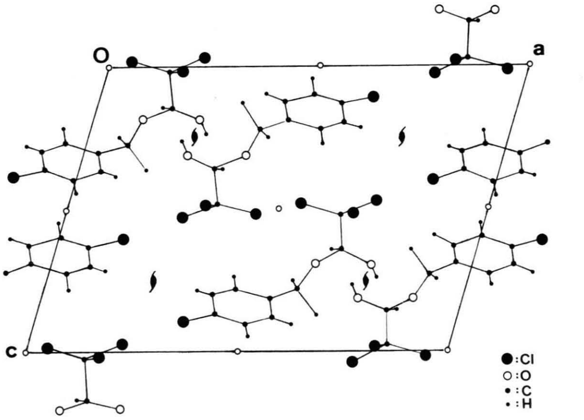

Fig. 3. The crystal structure of pCB-CH projected along the *b*-axis onto the (*ac*) plane.

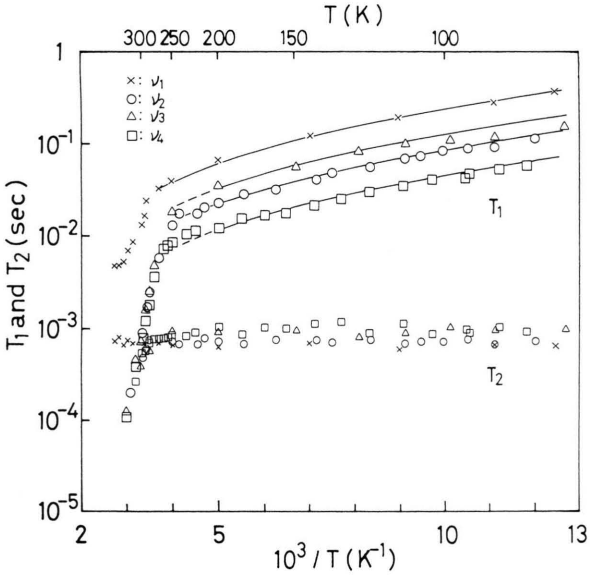

Fig. 4. The temperature dependence of T_1 and T_2 of ^{35}Cl NQR in pCB-CH. ν_1 and ν_{2-4} correspond to the Cl atom on the benzene ring and to those in CCl_3, respectively (see Fig. 1).

tal structure suggests the possibility of three models of hydrogen bond chains as shown in Figure 5.

According to the classification of intermolecular hydrogen bonds proposed by Jeffrey and Takagi [11], (a), (b), and (c) in Fig. 5 correspond to IA, IIB, and IIIA or IVA type hydrogen bond in carbohydrate, respectively. Model (c) corresponds to the three center hydrogen bond (so called bifurcated one). It is characteristic for pCB-CH that the intermolecular O2 ··· O1′ and O2 ··· O2′ distances (306.4 and 319.8 pm, respectively) are relatively long compared to the O ··· O distances for typical OH ··· O hydrogen bonds.

A dynamic disorder of hydrogen atoms in the hydrogen bond chain has been proposed as a probable source of the fluctuation of EFG responsible for the T_1 minimum of Cl NQR found for nB-CH and cycHx-CH [4, 5]. The intermolecular arrangement of the –CH(OH)–O– group in the hydrogen bond chain of pCB-CH is almost identical to those in nB-CH and cycHx-CH except for subtle differences in the intermolecular O ··· O distances (see Table 3). The similarity of the crystal structure and the splitting of the OH stretching band seem to support a disorder of H1 hydrogen atoms in pCB-CH. Moreover, the diffuse

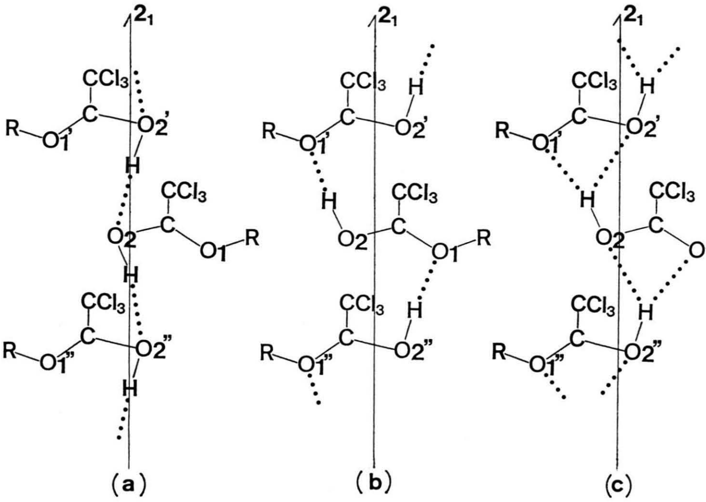

Fig. 5. Three models of hydrogen bond chains in the crystal of pCB-CH. The hydrogen atoms on the central carbon atoms are omitted for simplicity.

Table 3. Intermolecular O ··· O distances in the hydrogen bond chains of some chloral hemiacetals.

Compound	*d*(O2 ··· O1')/pm *	*d*(O2 ··· O2')/pm *
pCB-CH	307.4	319.8
cycHx-CH	304.4	324.0
nB-CH	296.7	322.8

* For the meaning of O2, O1' and O2', see Figure 5.

Table 4. The ^{35}Cl NQR frequencies at 90 K ($\nu(90)$) and the parameters (a, b, and E_a) of (1) and (2).

Line no.	$\nu(90)$/MHz	$10^3 a$	$10^{-12} b$	E_a/kJ mol^{-1}
ν_1	34.301	0.40 ± 0.01		
ν_2	38.547	1.13 ± 0.02	0.29 ± 0.03	48.3 ± 0.3
ν_3	38.826	0.76 ± 0.03	1.52 ± 0.65	52.8 ± 1.2
ν_4	39.442	2.14 ± 0.05	0.72 ± 0.23	50.4 ± 0.9

electron distribution suggests a disorder corresponding to a superposition of (b) and (c) models in Fig. 5, although discussion on the location of the hydrogen atom is limited in the X-ray work.

For pCB-CH, however, a T_1 minimum was not observed in the temperature range $80 \lesssim T/\mathrm{K} \lesssim 330$ K. This might indicate that the magnitude of the fluctuation of the EFG due to the disorder would be too small to produce an appreciable drop of T_1, or that the frequency spectrum of the molecular motion due to the dynamic disorder would be far apart from the NQR frequency in the temperature range investigated.

T_1 of ν_{2-4} (Cl NQR of CCl$_3$)

As usual, the temperature dependence of T_1^{-1} of ν_{2-4} is described approximately by the equations [12]

$$T_1^{-1} = \mathrm{a}\,\mathrm{T}^{2}, \qquad 80 \lesssim T \lesssim 200\ \mathrm{K}, \quad (1)$$

$$T_1^{-1} = b \exp(-E_a/RT), \qquad T \gtrsim 270\ \mathrm{K}. \quad (2)$$

The parameters, a, b, and E_a, are given in Table 4. Since in the lower temperature region the observed temperature dependence of T_1^{-1} obeys the T^2 law, the spin lattice relaxation is considered to be governed by lattice vibrations [12].

The sharp decrease in T_1 with increasing temperature observed above 260 K is attributable to the onset of reorientation of the CCl$_3$ group. The magnitudes of V_0 (50 ± 2 kJ/mol in average) obtained for ν_{2-4} are comparable to those reported for the reorientation [1].

Since intra- and intermolecular contacts between the CCl$_3$ group and the neighboring atoms are responsible for V_0, the atom-atom potential method is a way of estimating it. Then we calculated the atom-atom potential energy (U) as a function of rotation angle by rotating the CCl$_3$ group around its C_3 axis using the equation [13]

$$U = \sum \varepsilon_i (2.90 \times 10^5 \exp\{-12.50/P_i\} - 2.25\,P_i^6)\,, \quad (3)$$

where P_i stands for the sum of the van der Waals radii divided by the distance between interaction centers. The van der Waals radii and ε_i were taken from [13]. The intra- and intermolecular contributions to V_0 were calculated to be approximately 24 and 92 kJ/mol, respectively. Thus the latter contribution dominates the magnitude of V_0. The calculated value of V_0 (ca. 116 kJ/mol) is greater than the experimental one but a discussion of the absolute value of the calculated V_0 seems to be artificial because of its strong dependence on the parameters used in the calculation.

T_1 *of* ν_1 *(NQR of the Cl Atoms on Benzene Ring)*

In the range of $80 \lesssim T/\mathrm{K} \lesssim 270$, T_1^{-1} obeys (1) with the constant given in Table 4, indicating that the spin lattice relaxation of ν_1 is governed by lattice vibrations. At $T \gtrsim 280$ K, however, the temperature dependence of T_1^{-1} deviates from the T^2 law. Furthermore, T_1 seems to show a minimum at ca. 360 K. Since the Cl atom on the benzene ring (Cl4) is located near the CCl_3 group in the crystal, the reorientation of the group would affect the spin lattice relaxation of ν_1. But the rate of the reorientation at ca. 360 K is estimated to be too slow to explain the apparent T_1 minimum of ν_1. A study of the T_1 behavior above 280 K is now in progress.

[1] H. Chihara and N. Nakamura, Adv. Nucl. Quad. Resonance **4,** 1 (1980).

[2] M. Hashimoto, K. Hamada, and K. Mano, Bull. Chem. Soc. Japan **60,** 1924 (1987).

[3] M. Hashimoto, N. Nakamura, M. Adachi, K. Hamada, and K. Mano, Ber. Bunsenges. Phys., Chem. **93,** 439 (1989).

[4] M. Hashimoto, T. Isono, H. Niki, and T. Higa, Z. Naturforsch. **45 a,** 472 (1990).

[5] H. Niki, H. Kyan, T. Hamagawa, R. Igei, T. Isono, and M. Hashimoto, Z. Naturforsch. **47 a,** 299 (1992).

[6] Beilstein, Band I, S. 619.

[7] P. Main, S. E. Hull, L. Lessinger, G. Germain, J. P. Declercq, and M. M. Woolfson, MULTAN78, A System of Computer Programs for the Automatic Solution of Crystal Structures from X-ray Diffraction Data, University of York, England, and Louvain, Belgium 1978.

[8] T. Ashida, The Universal Crystallographic Computing Systems – Osaka, HBLS-V, p. 53. The Computer Center, Osaka University, Japan 1979.

[9] T. Sakurai and K. Kobayashi, Rikagaku Kenkyusho Hokoku **55,** 69 (1979).

[10] Y. Mido and M. Hashimoto, J. Mol. Struct. **129,** 253 (1985).

[11] G. J. Jeffrey and S. Takagi, Acc. Chem. Res. **1,** 264 (1978).

[12] D. E. Woessner and H. S. Gutowsky, J. Chem. Phys. **39,** 440 (1963).

[13] N. L. Allinger, J. Amer. Chem. Soc. **99,** 8127 (1977).